

# A NOVEL ELECTRON-BPM FRONT END WITH SUB-MICRON RESOLUTION BASED ON PILOT-TONE COMPENSATION: TEST RESULTS WITH BEAM

G. Brajnik\*, S. Carrato, University of Trieste, 34127 Trieste, Italy

S. Bassanese, G. Causero, R. De Monte, Elettra-Sincrotrone Trieste, 34149 Trieste, Italy

## Abstract

In this paper we present a novel and original four-channel front end developed for a beam position monitor (BPM) system. In this work, we demonstrate for the first time the continuous calibration of the system by using a pilot tone for both beam current dependency and thermal drift compensation, completely eliminating the need for thermoregulation. By using this approach, we were also able to investigate several odd and well-known behaviours of BPM systems; the influence of important issues, like the non-linearity of ADCs and the gain compression of amplifiers, which do affect the reliability of the measurement, have been fully understood. To achieve these results, we developed a new radio-frequency front end that combines the four pick-up signals originated by the beam with a stable and programmable tone, generated within the readout system. The signals from a button BPM of Elettra storage ring have been acquired with a 16-bit, 160 MS/s digitizer controlled by a CPU that evaluates the acquired data and applies the correction factor of the pilot tone. A final resolution equal to 1  $\mu\text{m}$ , for a vacuum chamber with an average radius of 19 mm, has been measured with a long-term stability better than 1  $\mu\text{m}$ .

## INTRODUCTION

Accuracy in BPM systems is strongly influenced by the following factors: beam current dependency (to achieve the proper dynamic range, the gains of the preamplifiers have to be adjusted), thermal drifts of electronics (filters, amplifiers, ADCs) and variations of the frequency response of the cables due to changes in temperature or humidity. All of these issues are responsible for inter-channel gain differences, which modify the calculated position.

Typically, every factor has its own compensation method: e.g. gain calibration look-up tables, thermal controlled racks, low-loss cables. The proposed strategy aims to correct all the factors simultaneously: a fixed sinusoidal tone (used as the same reference for all the channels) is added to the original signal coming from the beam (called carrier). A similar technique is already known [1–3], but for the first time experimental results have shown the improvement in resolution due to this method. In order to achieve an effective correction, the pilot tone frequency has to fall near the carrier one, without, however, interfering with the latter. The position of the tone is crucial: only the gaps between the beam harmonics (spaced by the inverse of revolution period) are suitable frequencies [4].

\* gabriele.brajnik@elettra.eu

## PROPOSED COMPENSATION

Let  $a(t)$  be the input signal coming from the beam,  $p(t)$  the pilot tone and  $h_A(t)$  the response of channel A. The output of the chain, after the coupler, the filter and the amplifier is a convolution:  $s_A(t) = h_A(t) * [a(t) + p(t)]$ . Moving to the frequency domain and using the Fourier transforms in calligraphy upper case, the output can be written as  $S_A(f) = \mathcal{H}_A(f) \cdot [\mathcal{A}(f) + \mathcal{P}(f)] = \mathcal{A}_M(f) + \mathcal{A}_P(f)$ , where  $\mathcal{A}_M(f) = \mathcal{H}_A(f) \cdot \mathcal{A}(f)$  and  $\mathcal{A}_P(f) = \mathcal{H}_A(f) \cdot \mathcal{P}(f)$ . The complete evaluation of  $\mathcal{H}_A(f)$ , if  $\mathcal{P}(f)$  is used, is not required if we suppose that  $f_P$  (the pilot frequency) and  $f_C$  (the carrier frequency) are close to each other, allowing us to write  $\mathcal{H}_A(f_P) \approx \mathcal{H}_A(f_C)$ . In this case, it can be written:

$$\mathcal{A}(f_C) = \frac{\mathcal{A}_M(f_C)}{\mathcal{H}_A(f_C)} = \frac{\mathcal{A}_M(f_C)}{\mathcal{A}_P(f_P)} \cdot \mathcal{P}(f_P) \quad (1)$$

Extracting the amplitudes from  $\mathcal{A}(f_C)$  for each channel and substituting them in the typical difference-over-sum (DoS) equation [5, 6] render it possible to calculate compensated spatial coordinates corrected for variations or mismatches of the preamplifiers:

$$X = L \cdot \frac{(A_M/A_P + D_M/D_P) - (B_M/B_P + C_M/C_P)}{A_M/A_P + B_M/B_P + C_M/C_P + D_M/D_P} \quad (2)$$

$$Y = L \cdot \frac{(A_M/A_P + B_M/B_P) - (C_M/C_P + D_M/D_P)}{A_M/A_P + B_M/B_P + C_M/C_P + D_M/D_P} \quad (3)$$

where  $A_M, B_M, C_M, D_M$  are the amplitudes of the measured carrier and  $A_P, B_P, C_P, D_P$  are the amplitudes of the pilot tone.

Obviously, to obtain a continuous and effective correction, care must be taken in treating the analog signals, as well as choosing appropriate computing power to digitally demodulate both carrier and pilot.

## ANALOG RF FRONT END

Figure 1 shows the block diagram of the system: a low-phase-noise PLL generates the pilot tone (whose frequency and amplitude are programmable), which is split into four paths by a high-reverse-isolation splitter that guarantees more than 52 dB of separation between the outputs. A coupler sums the tone with the signal from the pick-ups, adding further 25 dB of isolation to prevent inter-channel crosstalk from the path of the pilot tone. At this point, all the signals pass through a bandpass filter, centered at 500 MHz

with a bandwidth of 15 MHz, and two variable-gain stages, composed of low-noise, high-linearity amplifiers ( $G=22$  dB,  $F=0.5$  dB,  $OIP3=+37$  dBm,  $P1dB=+22$  dBm) and digitally controlled attenuators (7 bits, up to 31.75 dB of attenuation, steps of 0.25 dB).

In order to achieve the expected results, the splitter must be temperature-insensitive, as well as the four couplers. Indeed, this architecture allows us to compensate the part of the system after the couplers, i. e. filters, attenuators, amplifiers. It has to be noted that being the front end a separate unit, it can be placed as near as possible to the pick-ups (tunnel area), with two main advantages: better signal-to-noise ratio and the possibility to compensate the cables (which are usually long).

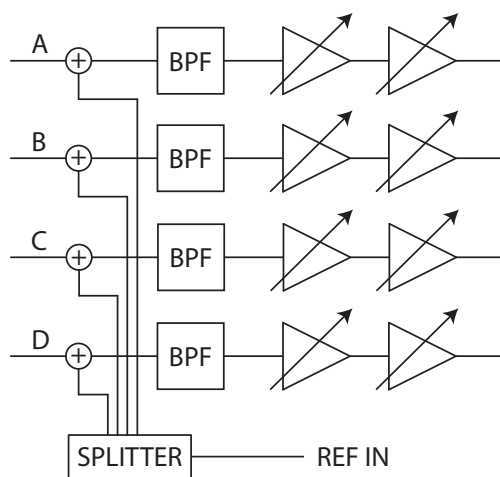


Figure 1: Block diagram of the RF front end.

## MEASUREMENT SETUP

The RF front end has been placed in Elettra tunnel area and connected to a button BPM of the storage ring (the average radius of the chamber is about 19 mm). Four cables of about 20 meters deliver the amplified signals to an in-house assembled digitizer (16 bit, 160 MS/s) located in the service area, that undersamples the 499.654 MHz carrier and the 504.6 MHz pilot tone respectively at 19.654 MHz and 24.6 MHz. The raw data stream from the ADCs is collected by an FPGA and transmitted via an Ethernet link without any processing. The position is calculated offline, so that the FFT of each channel provides the amplitude of the carrier and the pilot.

A clock conditioner with two cascaded PLLs ensures the correct synchronization of the system with the storage-ring clock (1.156 MHz) and generates both a low-jitter sampling clock (measured to be around 100 fs), a fundamental condition for undersampling applications, and a reference clock for the pilot-tone synthesizer.

ISBN 978-3-95450-177-9

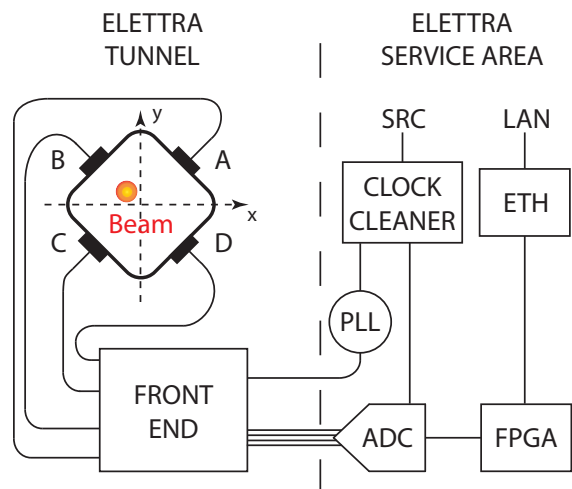


Figure 2: Block diagram of the setup.

## INVESTIGATED ISSUES

With this setup (Figure 2), numerous sets of data have been acquired to understand several issues that affect the reliability of the measurement.

### Temperature Dependence

Thanks to four sensors placed on every ADC and one in the front-end box, a strong dependence between temperature and the amplitude of the signals (and so the position) has been found.

Simulating a centered and stable beam with a splitter that divides a real signal from a storage ring button BPM, it can be shown that identical thermal drifts affect the carrier and the pilot (figure 3); the compensation greatly improves the standard deviation of the position, from 1.26  $\mu\text{m}$  to 0.54  $\mu\text{m}$  in a 24-hours time window, allowing us to separate it into two contributions: the part due to temperature variation and the actual resolution of the measurement.

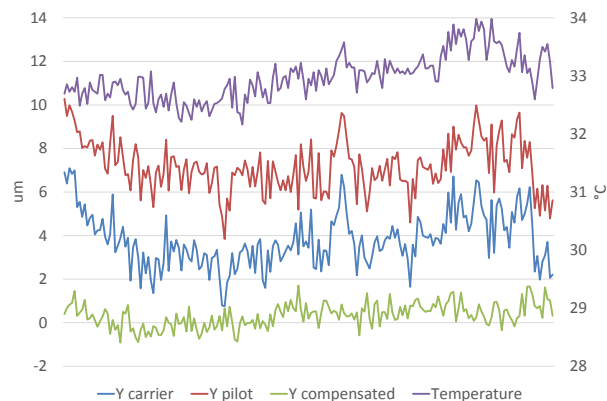


Figure 3: Changes in temperature and positions in a 24-hours time window.

### Gain Compression

According to their datasheet, the low-noise amplifiers have a high 1dB compression point, but the high sensitivity of the position algorithm shows compression effects of 0.1dB at a lower input level. A technique to prevent it is to bias the amplifiers at an appropriate point; anyway, supposing the carrier saturates the amplifier, the pilot level decreases in a very similar way, so the loss can be recovered using the compensation.

### Non-linearity of ADCs

It is well known that the transfer characteristic of ADCs suffers from non-linearity errors: the critical factor in our case is the integral non-linearity (INL). In order to evaluate these phenomena, we use the pilot tone as a fixed and stable beam. So, changing its global amplitude (but not among the channels), should keep the position almost in the same point thanks to the normalization made by the DoS.

Indeed, moving on the characteristic curve of the ADCs (input voltage vs. output code), discontinuities appear in the amplitudes digitized by the ADCs and obviously in the position. These discrepancies are about 110  $\mu\text{V}$  in amplitude, which correspond to the INL of the used ADCs, nominally 4-5 LSB.

Again, given that the signal coming from the beam is added to the pilot tone, the latter can be used to coerce the working range of the ADCs. If a small signal is coming from the beam, a higher pilot allows us to shift it in a more suitable zone of the transfer characteristic.

## RESULTS WITH BEAM

The following results have been collected with Elettra storage ring running in normal operation, 2.0 GeV and 310 mA. The BPM pick-ups used are close to an insertion device and between two bellows. The bellows assure the mechanical decoupling from the rest of the machine vacuum chamber. The beam orbit is kept stable at the center position by the global feedback. The input signal coming from the beam is -6 dBm, carrier and pilot amplitudes measured at the ADCs input are both 0 dBm, for a total amplitude of +6 dBm, that corresponds at the 80% of the ADCs working range.

The intrinsic resolution of the system has been measured in about 150 nm, using the pilot as a stable reference, an FFT of 2.4 MS and a chamber radius of 19 mm, .

First of all, we want to evaluate the influence of the pilot on the calculated position without compensation: no changes have been seen switching on and off the tone.

Subsequently, a single bunch has been injected to obtain a hybrid filling pattern. Also in this case the bunch does not affect in a significant way the position. Figure 4 shows the front-end output with a single bunch in the gap between two trains of bunches: the filter impulse response can be clearly seen.

Deliberate beam movements have been performed, with steps of 1  $\mu\text{m}$  and 10  $\mu\text{m}$ : the positions calculated by the sys-

tem have been reported in Table 1, where the compensation shows an improvement of 2.5  $\mu\text{m}$ .

Nevertheless, compensation is also useful for long-term stability. Figure 5 illustrates beam position in a 24-hours time window with and without correction: the standard deviation is reduced by a factor of two, from 1.36  $\mu\text{m}$  to 0.76  $\mu\text{m}$ , always considering an average chamber radius of 19 mm.

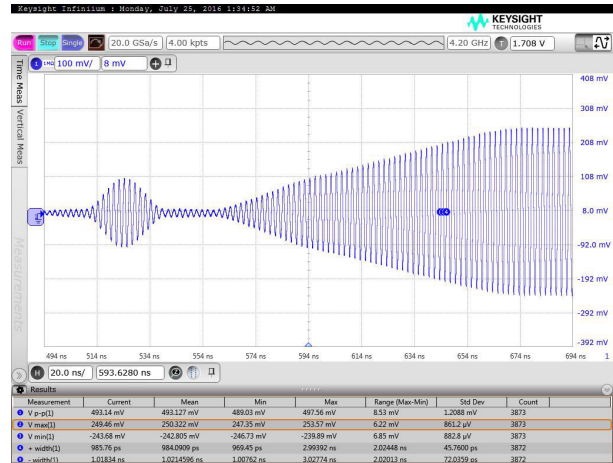


Figure 4: Front end output with a hybrid filling pattern: single bunch in the gap.

Table 1: Vertical Beam Movements

Actual movements	Measured position	
	Uncompensated	Compensated
+1 $\mu\text{m}$	+0.5 $\mu\text{m}$	+1.0 $\mu\text{m}$
-1 $\mu\text{m}$	-2.5 $\mu\text{m}$	-1.1 $\mu\text{m}$
+10 $\mu\text{m}$	+8.4 $\mu\text{m}$	+9.2 $\mu\text{m}$
-10 $\mu\text{m}$	-12.6 $\mu\text{m}$	-10.1 $\mu\text{m}$

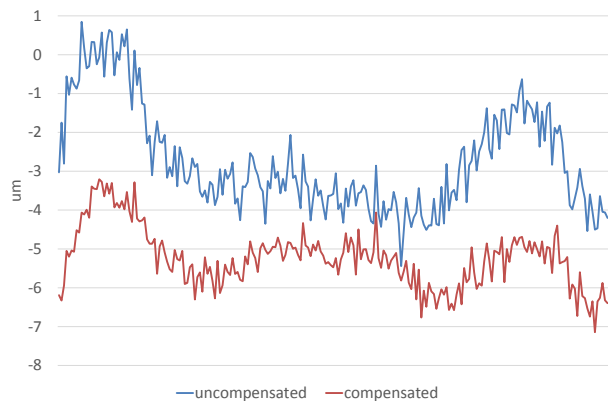


Figure 5: Beam Y-position in a 24-hours time window.

## CONCLUSION

In this paper, a novel RF front end for electron beam position monitors capable of sub-micron resolution and continuous calibration has been presented. Several tests confirm the

effectiveness of the compensation by using a pilot tone coupled with the signal coming from the beam: this approach can correct inter-channel gain mismatches and thermal drifts, without using thermal regulators. Moreover, the experience with this system helped us to better understand a number of issues that affect data acquisition in the BPM field.

Further developments are under way, in both hardware and software: an FPGA Mezzanine Card (FMC) with four 16-bit, 210 MS/s ADCs is ready to be tested and linked with an FPGA. Improvements will be made on the front end, by handling the automatic gain control (AGC) of the preamplifiers, by adding an amplification stage to recover cable losses and by considering a pilot-frequency hopping scheme to increase the compensation efficiency.

The position calculation and compensation will be implemented in the FPGA: two digital receivers will demodulate the signals, extracting the amplitudes of the carrier and of the pilot at the same time after decimation and additional filtering. At this point, just before the calculation of the position with the traditional difference-over-sum equation, the system will be able to apply or not the compensation, allowing the users to evaluate its effectiveness.

## REFERENCES

- [1] M. Dehler, *et al.*, "New digital BPM System for the Swiss Light Source", *Proceedings of DIPAC 1999*, pp. 168-170.
- [2] R. Baron, F. Cardoso, J. Neto, S. Marques and J. Denard, "Development of the RF Front-End Electronics for the Sirius BPM System", *Proceedings of IBIC 2013*, p. 670.
- [3] J. Mead, *et al.*, "NSLS-II RF Beam Position Monitor Commissioning Update", *Proceedings of IBIC 2014*, pp. 500-504.
- [4] G. Brajnik, S. Carrato, S. Bassanese, G. Cautero and R. De Monte, "Pilot tone as a key to improving the spatial resolution of eBPMs", *AIP Conference Proceedings*, vol. 1741, p. 020013 (2016).
- [5] R. E. Shafer, "Beam position monitoring", *AIP Conference Proceedings*, vol. 212, pp. 26-58 (1989).
- [6] P. Forck, P. Kowina and D. Liakin, "Beam position monitors", *CERN accelerator school on beam diagnostics*, pp. 187-228 (2008).